

## Supplementary Information

### Surface reconstruction of AgPd and AgPdF nanoalloys under the formate oxidation reaction

Quan Tang <sup>a,b</sup>, Fuyi Chen <sup>\*,a,b</sup>, Qiao Wang <sup>a,b</sup>, Tao Jin <sup>a,b</sup>, Longfei Guo <sup>a,b</sup>, Ying Wu <sup>a,b</sup>, Shangjia Yu <sup>a,b</sup> and Zhen Li <sup>a,b</sup>

a. State Key Laboratory of Solidification Processing, Northwestern Polytechnical University, Xian, 710072, China.

b. School of Materials Science and Engineering, Northwestern Polytechnical University, Xi'an, 710072, China.

\*Corresponding author: fuyichen@nwpu.edu.cn (Fuyi Chen)

**Table S1** The EDS compositions for various AgPd nanoalloys with different molar ratios of metal precursors during the synthetic process compared with monometallic counterparts.

AgNO <sub>3</sub> (mM)	H <sub>2</sub> PdCl <sub>4</sub> (mM)	EDS composition (wt %)		Atomic ratio (%)	
		Ag	Pd	Ag/Pd	
Pd	0	40	0	100	0/100
	10	30	28.8	71.2	29/71
<b>AgPd</b>	<b>20</b>	<b>20</b>	<b>50.4</b>	<b>49.6</b>	<b>50/50</b>
	30	10	76.7	23.3	76/24
Ag	40	0	100	0	100/0

**Table S2** The EDS compositions for various AgPdF nanoalloys with different concentrations of NH<sub>4</sub>F during the synthesis compared with AgPd nanoalloy.

Nanoalloys	T (K)	Concentration of NH <sub>4</sub> F (mM)	EDS composition (wt %)			Atomic ratio (%) Ag/Pd/F
			Ag	Pd	F	
AgPd		0	50.4	49.6	0	50/50/0
	353	20	51.2	48.5	0.3	50/48/2
	<b>353</b>	<b>40</b>	<b>51</b>	<b>48.4</b>	<b>0.6</b>	<b>49/47/4</b>
	353	60	50.8	48.3	0.9	47/47/6
	353	80	50.7	48.2	1.1	46/47/7

**Table S3** A literature survey of the catalytic activity of Pd-based and Pt-based FOR catalysts in alkaline media.

Catalyst	Electrolyte	Scan rate (mV·s <sup>-1</sup> )	Specific activity (mA·cm <sup>-2</sup> )	Mass activity (A·mg <sub>Pd</sub> <sup>-1</sup> )	Reference
<b>AgPdF</b>	<b>1.0 M KOH + 1.0 M HCOOK</b>	<b>50</b>	<b>20.5</b>	<b>2.3</b>	<b>This work</b>
PdH/C	1.0 M KOH + 0.1 M HCOOK	20	0.1	NA	1
Pd <sub>4</sub> Ag/C	1.0 M NaOH + 0.1 M HCOONa	50	NA	0.04	2
PdCu/C	1.0 M KOH + 1.0 M HCOOK	30	3.5	NA	3
PdAu/Ni foam	0.5 M NaOH + 0.1 M HCOONa	50	0.8	NA	4
Ag <sub>49</sub> Pd <sub>51</sub> /rGO	1.0 M KOH + 1.0 M HCOOK	50	4.1	4.2	5
CuPdAu/C	0.5 M KOH + 0.5 M HCOOK	50	NA	1.2	6
PdAgCu aerogels	1.0 M KOH + 1.0 M HCOOK	50	10.1	2.7	7
PdAgPt aerogels	0.5 M KOH+ 0.5 M HCOOK	50	3.5	2.9	8
Pd <sub>3</sub> Au <sub>3</sub> Ag <sub>1</sub> /CNT	1.0 M KOH + 1.0 M HCOOK	50	14.3	4.5	9
janus-Ag <sub>20</sub> Pd <sub>60</sub> Ni <sub>20</sub>	1.0 M KOH + 1.0 M HCOOK	50	7.4	1.3	10
Pd <sub>55</sub> Ag <sub>30</sub> Rh <sub>15</sub> /C	1.0 M KOH + 1.0 M HCOOK	50	3.0	1.9	11
Pd <sub>6</sub> Ag <sub>3</sub> Ru <sub>1</sub> /pCNTs	1.0 M KOH + 1.0 M HCOOK	50	NA	4.7	12
PdAgIr NFs/C	1.0 M KOH + 1.0 M HCOOK	50	6.5	4.4	13
Ag <sub>30</sub> Pd <sub>69</sub> Co <sub>1</sub> H-NSS	1.0 M KOH + 1.0 M HCOOK	50	16.9	3.1	14
Pd <sub>72</sub> Ce <sub>28</sub> /C	1.0 M KOH + 1.0 M HCOOK	50	19.4	1.1	15
Pd <sub>2.3</sub> Co/C	1.0 M KOH + 1.0 M HCOOK	50	NA	2.5	16
PdNi/C	1.0 M KOH + 1.0 M HCOOK	50	12.0	4.5	17
PdRh/C	1 M KOH + 1.0 M HCOOK	50	8.1	4.5	18
Pt-Ag	1 M KOH+ 1.0 M HCOOK	50	NA	0.8	19

**Table S4** The XPS surface composition of element Ag in the AgPdF, AgPdO and AgPd catalysts and the pure Ag counterpart.

Catalysts	Ag			Ag(I)		
	3d <sub>5/2</sub>	3d <sub>3/2</sub>	Total	3d <sub>5/2</sub>	3d <sub>3/2</sub>	Total
Ag	BE (eV)	367.9	373.9		369.0	374.8
	Content (%)	58.3	38.3	96.6	1.9	1.5
AgPd	BE (eV)	368.1	374.1		369.4	375.2
	Content (%)	57.3	37.5	94.8	3.4	1.8
AgPdO	BE (eV)	368.2	374.1		368.9	374.9
	Content (%)	46.7	33.3	80	11.9	8.1
AgPdF	BE (eV)	368.2	374.2		369.3	374.6
	Content (%)	39.8	30.2	70	20.3	9.7

BE: XPS binding energy.

**Table S5** The XPS surface composition of element Pd in the AgPdF, AgPdO and AgPd catalysts and the pure Pd counterpart.

Catalysts	Pd			Pd(II)		
	3d <sub>5/2</sub>	3d <sub>3/2</sub>	Total	3d <sub>5/2</sub>	3d <sub>3/2</sub>	Total
Pd	BE (eV)	335.7	341.0		336.5	342.6
	Content (%)	45.8	34.4	80.2	12.6	7.2
AgPd	BE (eV)	335.4	340.7		336.5	342.0
	Content (%)	52.9	35.7	88.6	6.7	4.7
AgPdO	BE (eV)	335.1	340.4		336.2	341.1
	Content (%)	53.9	38.5	92.4	4.8	2.8
AgPdF	BE (eV)	335.5	340.9		336.6	342.1
	Content (%)	51	36.7	87.7	7.9	4.4
						12.3

## BE: XPS binding energy.

**Table S6** Adsorption energies, potential limiting barriers, activation barriers and catalytic activities on the AgPdF(111) surface compare to AgPdO(111), AgPd(111), Pd(111) and Ag(111) surfaces.

Surfaces	Adsorption energy (eV)				$\Delta G$ (eV)	$E_{act}$ (eV)	Catalytic activity (A·mg <sub>Pd</sub> <sup>-1</sup> )
	HCOO	OH	H	CO <sub>2</sub>			
Ag(111)	-1.63	-1.72	-1.91	-0.07	0.8	0.96	0
Pd(111)	-2.01	-2.05	-2.71	-0.58	0.69	0.87	0.4
AgPd(111)	-1.95	-1.98	-2.46	-0.35	0.62	0.77	0.5
AgPdO(111)	-2.33	-2.46	-1.36	-0.32	0.56	0.72	1.3
<b>AgPdF(111)</b>	<b>-2.54</b>	<b>-2.75</b>	<b>-1.32</b>	<b>-0.3</b>	<b>0.36</b>	<b>0.66</b>	<b>2.3</b>

$\Delta G$  denotes the change of free energy for the potential-limiting step, and  $E_{act}$  denotes the activation energy for HCOO decomposition reaction.

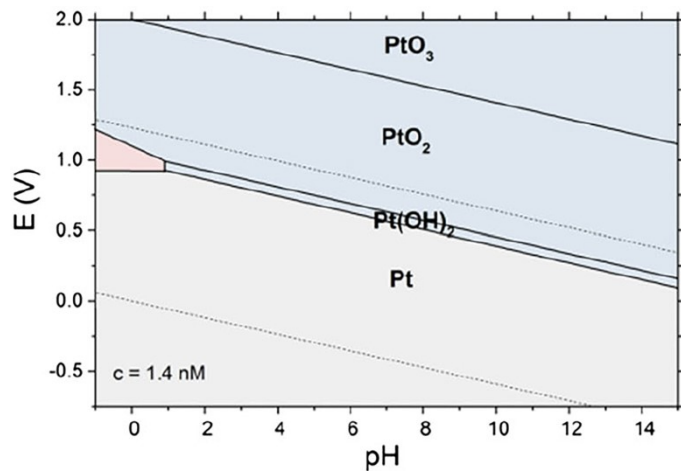


**Figure S1** Pourbaix diagram for the electrochemical equilibria of Pt in aqueous non-complexing electrolyte.<sup>20</sup> Grayish shaded areas: immunity against corrosion. Blue shaded area: formation of stable oxides. Reddish marked area: dissolution.

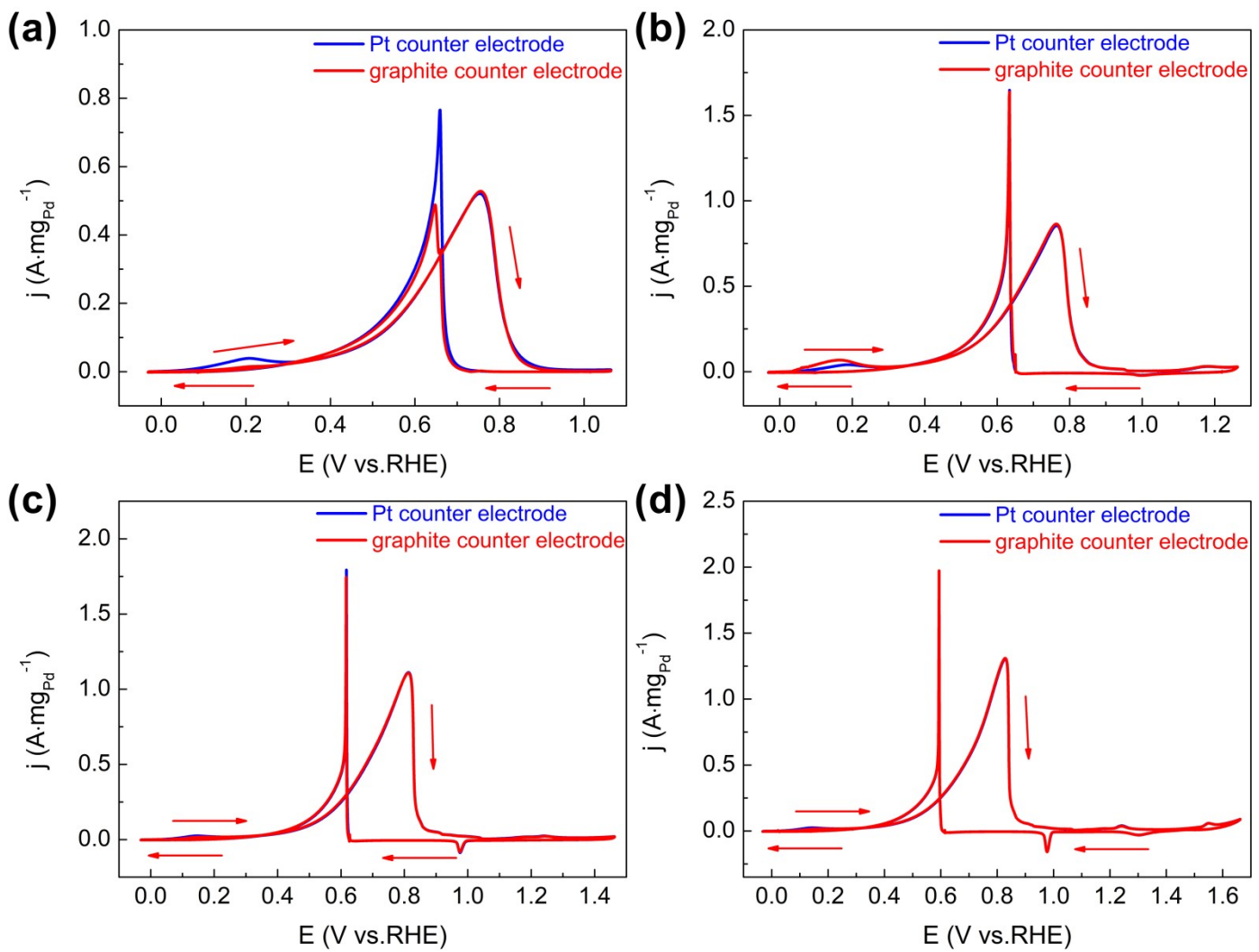


**Figure S2** Cyclic voltammetry (CV) curves of the AgPd catalyst with the upper limit potentials of 1.1 V (a), 1.3V (b), 1.5 V (c) and 1.7 V (d) at a scan rate of  $50 \text{ mV}\cdot\text{s}^{-1}$  in  $\text{N}_2$ -saturated 1 M KOH with 1 M HCOOK solution normalized by the mass of Pd. The blue lines are the CV curves measured with Pt counter electrode, and the red lines are the CV curves measured with graphite counter electrode.

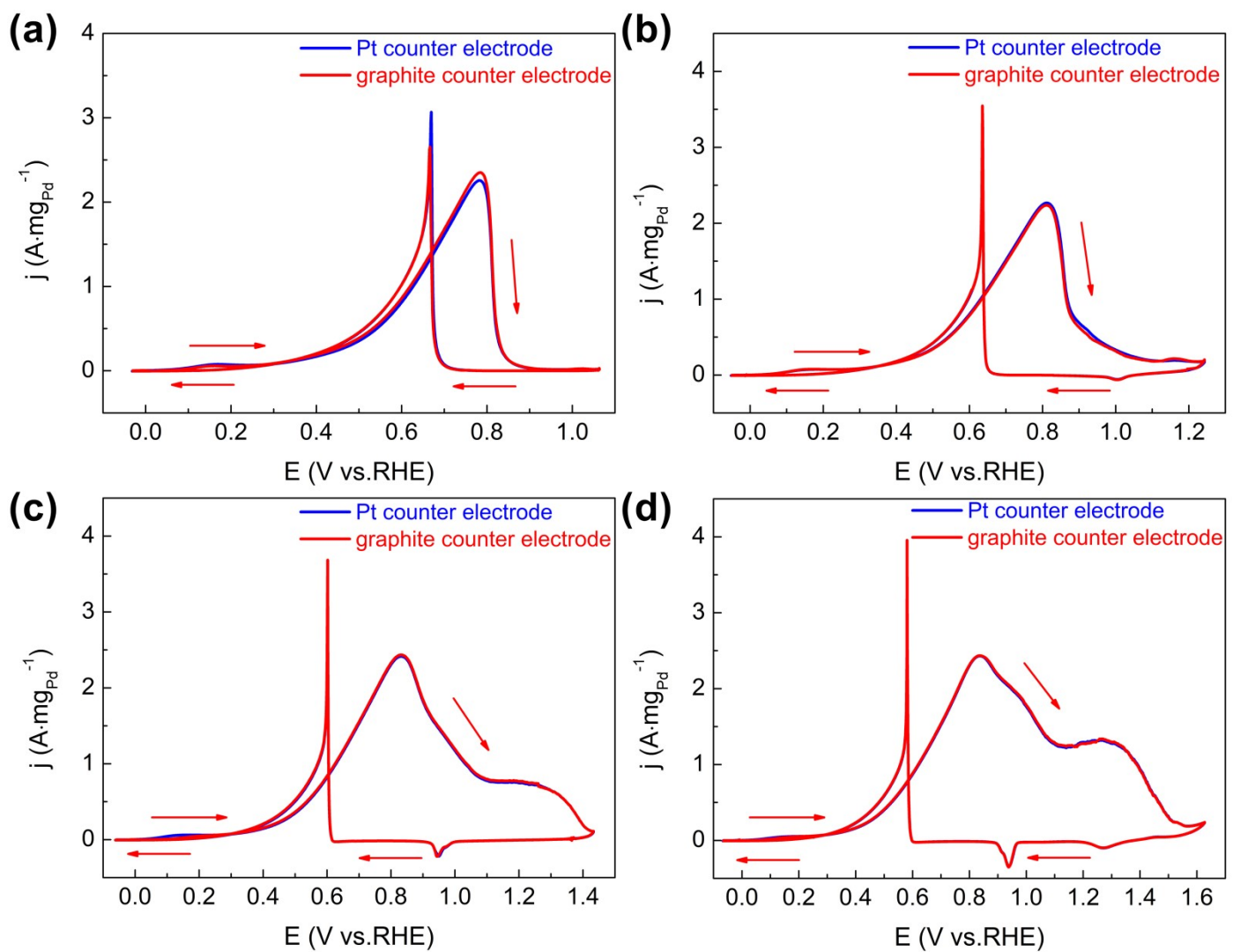


**Figure S3** CV curves of the AgPdF catalyst with the upper limit potentials of 1.1 V (a), 1.3V (b), 1.5 V (c) and 1.7 V (d) at a scan rate of  $50 \text{ mV} \cdot \text{s}^{-1}$  in  $\text{N}_2$ -saturated 1 M KOH with 1 M HCOOK solution normalized by the mass of Pd. The blue lines are the CV curves measured with Pt counter electrode, and the red lines are the CV curves measured with graphite counter electrode.

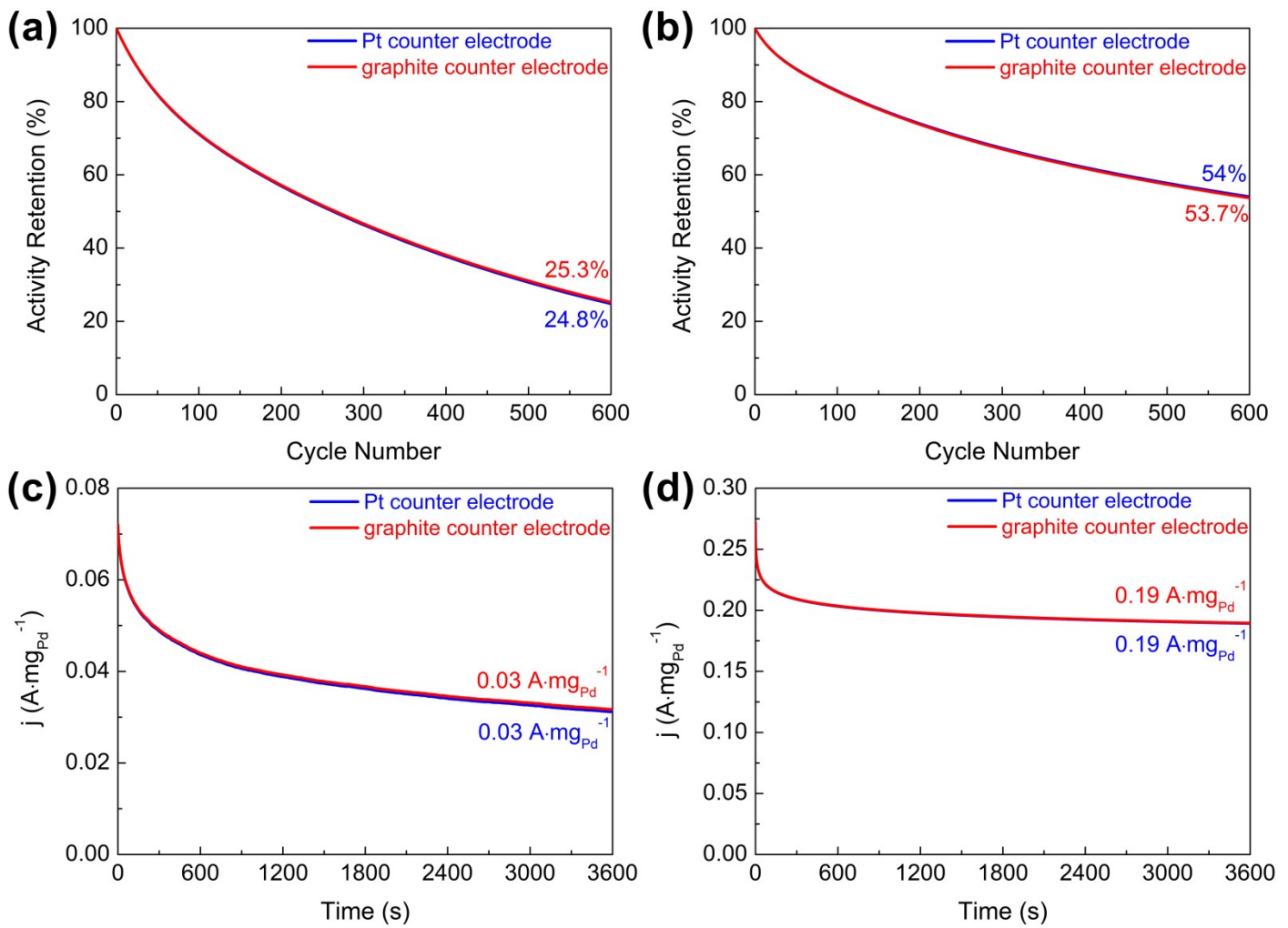


**Figure S4** Activity retention within 600 CV cycles of AgPd (a) and AgPdF (b) catalysts at the upper limit potentials of 1.1 V. Chronoamperometry (CA) curves at 0.45 V of AgPd (c) and AgPdF (d) catalysts for 3600 s. The blue lines are the curves measured with Pt counter electrode, and the red lines are the curves measured with graphite counter electrode.

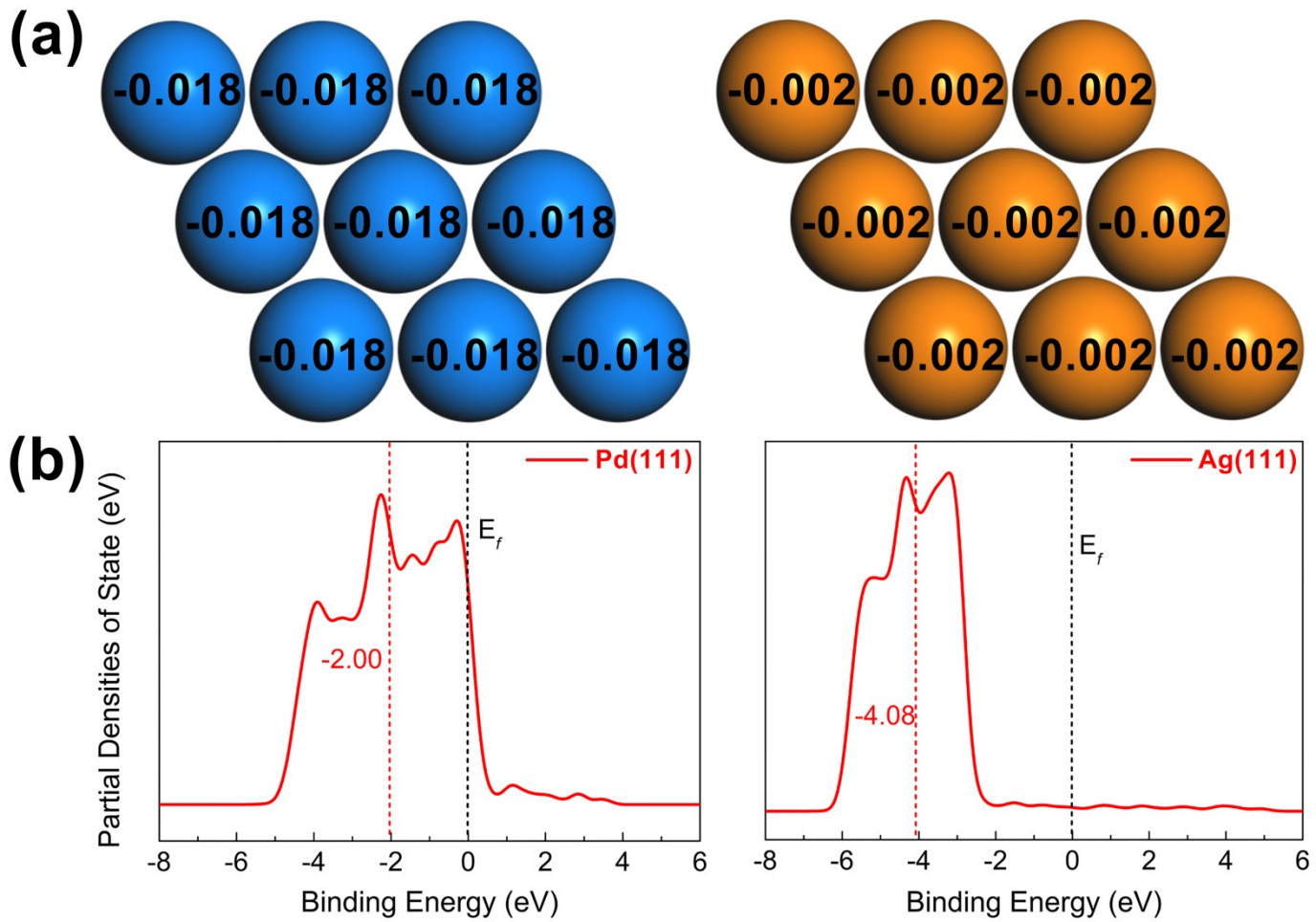


**Figure S5** (a) Mulliken atomic charge distribution on Pd(111) and Ag(111) surfaces. (b) Partial densities of state (PDOS) of Pd(111) and Ag(111) surfaces. The dashed lines vertical to the x-axis represent the d-band centers and Fermi level, respectively.

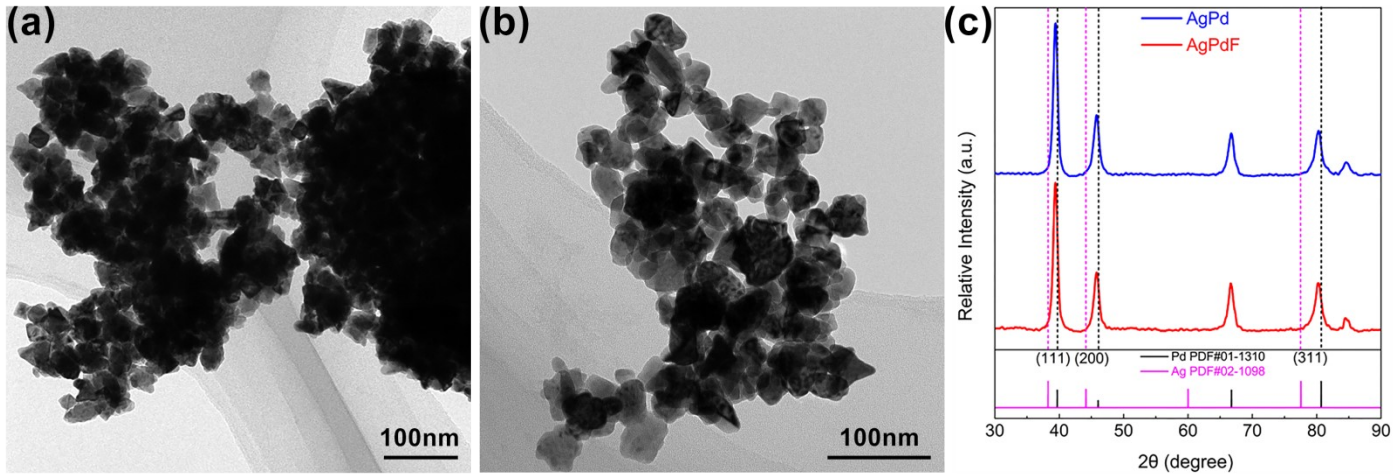


**Figure S6** Low-magnification TEM images of (a) AgPd and (b) AgPdF nanoalloys. (c) Full-range XRD patterns of AgPdF and AgPd nanoalloys, the standard XRD patterns for Ag and Pd are also provided for reference.

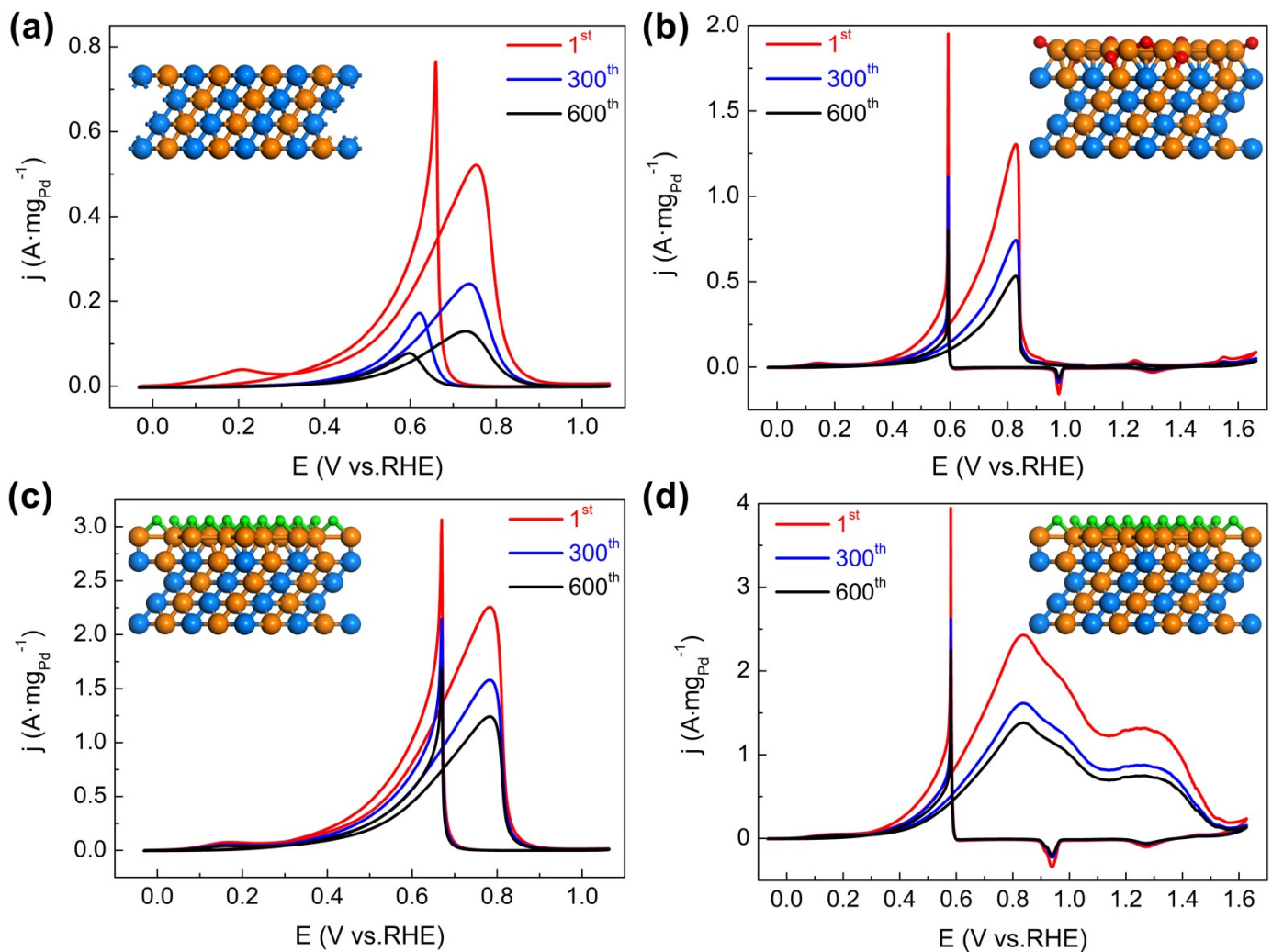


**Figure S7** CV curves in 1<sup>st</sup>, 300<sup>th</sup> and 600<sup>th</sup> cycles of the AgPd (a), AgPdO (b), AgPdF catalysts with the upper limit potentials of 1.1 V (c) and 1.7 V (d) at a scan rate of 50 mV·s<sup>-1</sup> in N<sub>2</sub>-saturated 1 M KOH with 1 M HCOOK solution normalized by the mass of Pd.

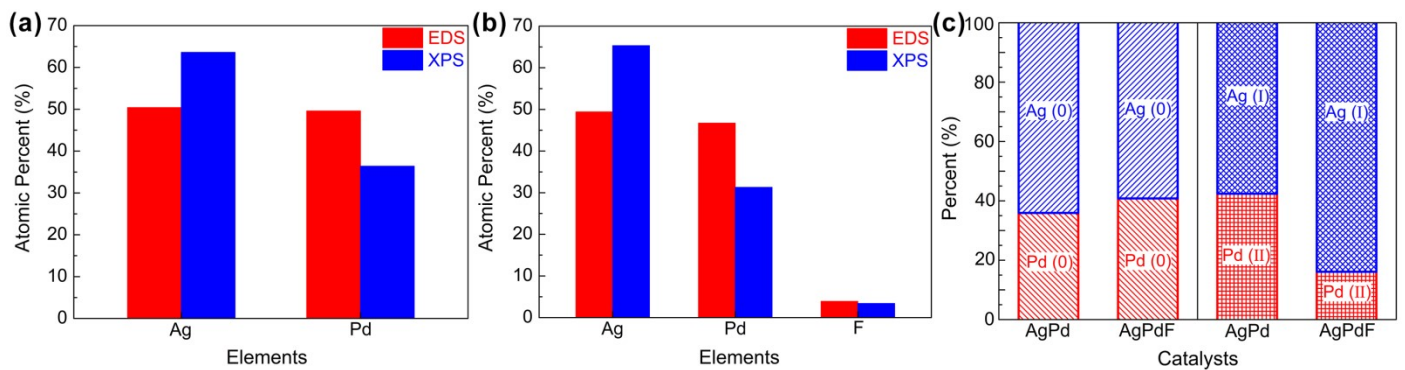


**Figure S8** The comparison for the bulk composition from EDS and the surface composition from XPS of (a) AgPd and (b) AgPdF catalysts. (c) The comparison for the Ag, Pd, Ag(I) and Pd(II) composition from XPS between AgPdF and AgPd catalysts.

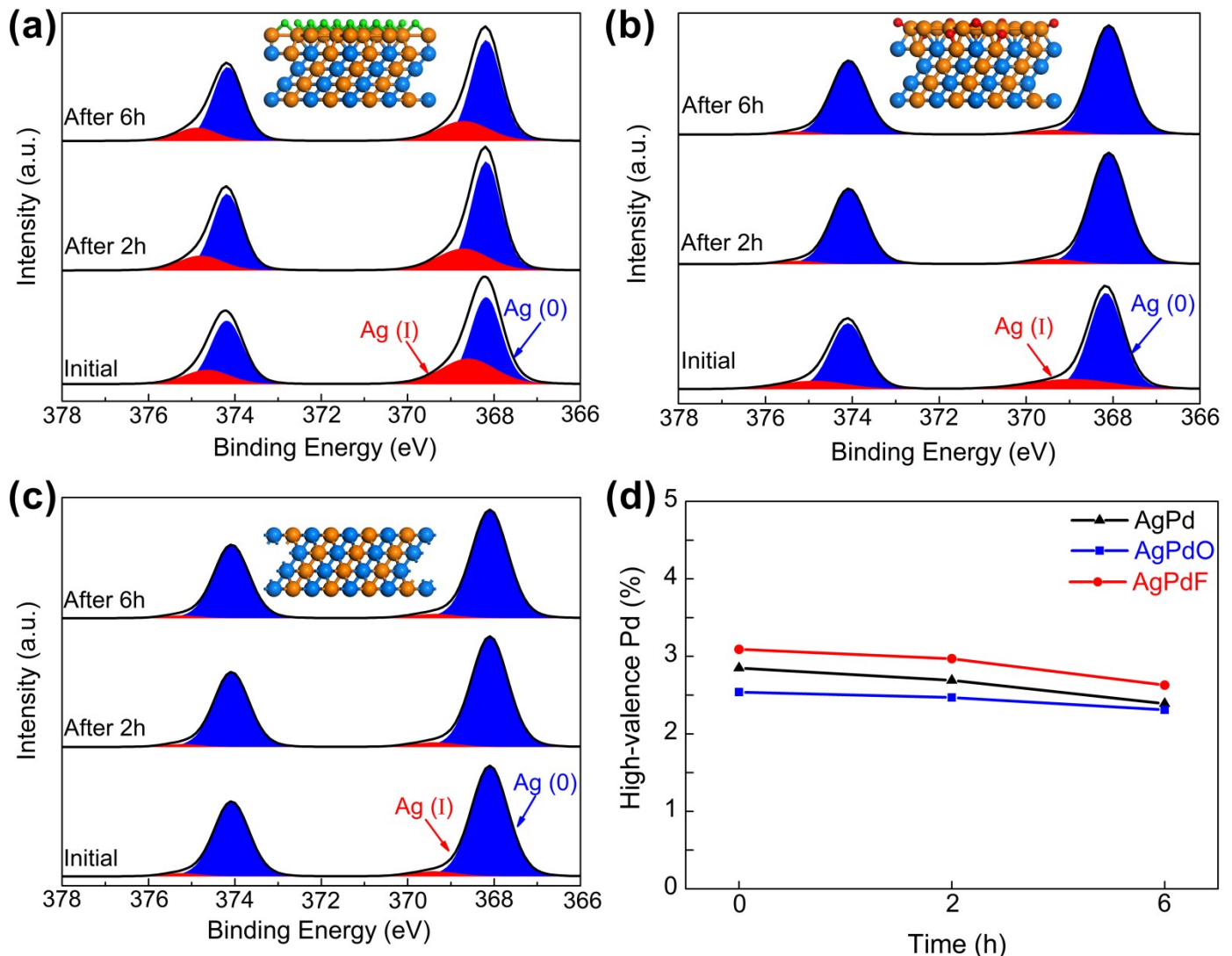


**Figure S9** High-resolution XPS spectrum of Ag 3d in (a) AgPdF, (b) AgPdO and (c) AgPd catalysts of the initial state, after 2 h CA test and after 6 h CA test. (d) Surface compositional comparison of high-valence metal Pd(II) in the AgPdF, AgPdO and AgPd catalysts of the initial state, after 2 h CA test and after 6 h CA test.

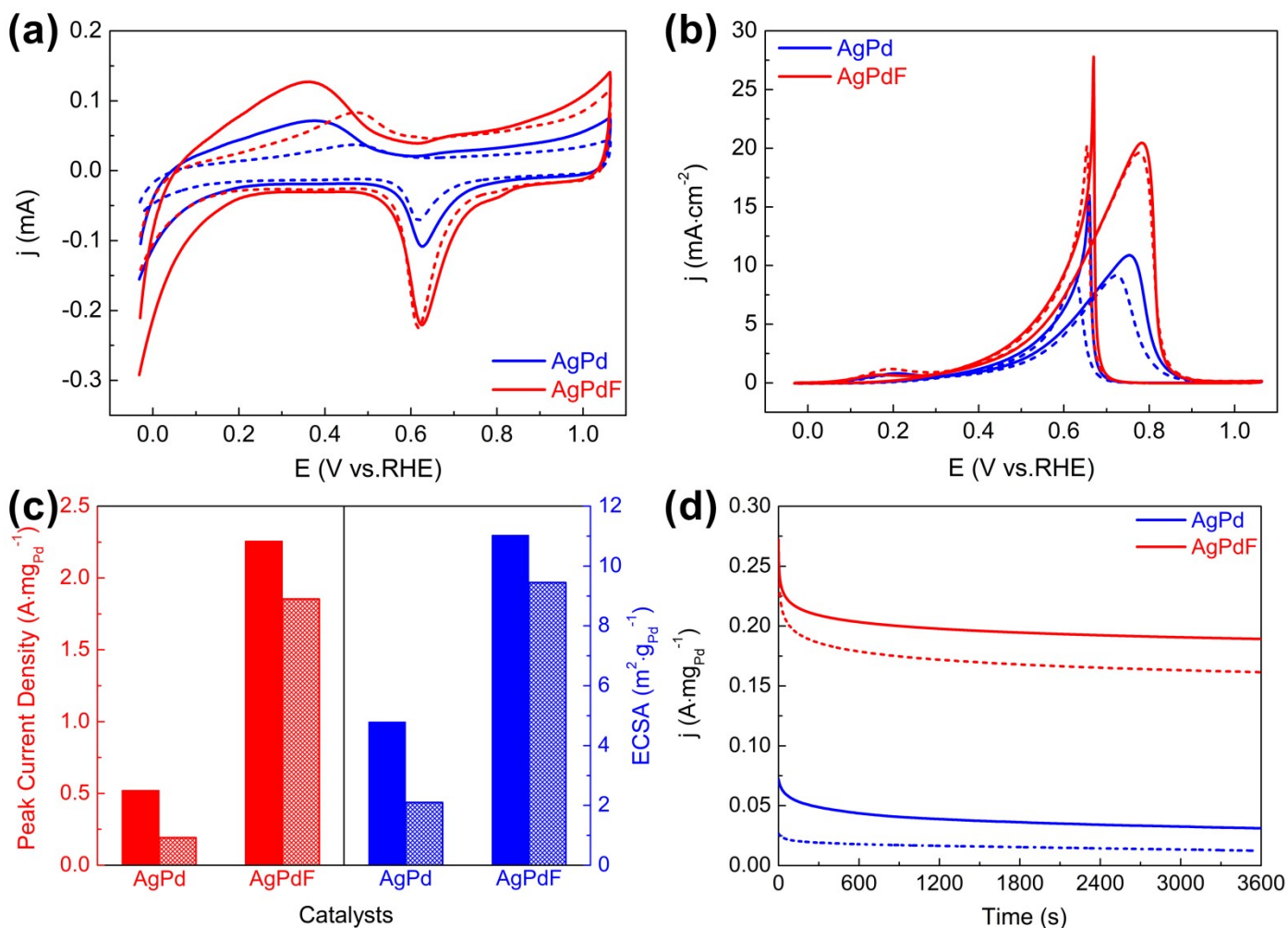


**Figure S10** Electrochemical performance of the AgPdF and AgPd catalysts after the immersion for the FOR. CV curves of the AgPdF and AgPd catalysts before and after the immersion at a scan rate of  $50 \text{ mV} \cdot \text{s}^{-1}$  in  $\text{N}_2$ -saturated 1 M KOH solution (a) and 1 M KOH with 1 M HCOOK solution normalized by the ECSA (b). (c) The comparison of the peak current density normalized by the mass of Pd and the ECSA of the AgPdF and AgPd catalysts before and after the immersion. (d) CA curves of various catalysts at 0.45 V in  $\text{N}_2$ -saturated 1 M KOH with 1 M HCOOK solution.

## Reference

1. M. Choun, K. Ham, D. Shin, J. K. Lee and J. Lee, *Catalysis Today*, 2017, **295**, 26-31.
2. S. Roy Chowdhury, S. Ghosh and S. K. Bhattacharya, *Electrochimica Acta*, 2017, **225**, 310-321.
3. J. Noborikawa, J. Lau, J. Ta, S. Hu, L. Scudiero, S. Derakhshan, S. Ha and J. L. Haan, *Electrochimica Acta*, 2014, **137**, 654-660.
4. Y. Li, Y. He and W. Yang, *Journal of Power Sources*, 2015, **278**, 569-573.
5. L. Guo, F. Chen, T. Jin, H. Liu, N. Zhang, Y. Jin, Q. Wang, Q. Tang and B. Pan, *Nanoscale*, 2020, **12**, 3469-3481.
6. H. Mao, T. Huang and A. Yu, *International Journal of Hydrogen Energy*, 2016, **41**, 13190-13196.
7. Q. Wang, F. Chen, L. Guo, T. Jin, H. Liu, X. Wang, X. Gong and Y. Liu, *J. Mater. Chem. A*, 2019, **7**, 16122-16135.
8. J. Wang, F. Chen, Y. Jin, L. Guo, X. Gong, X. Wang and R. L. Johnston, *Nanoscale*, 2019, **11**, 14174-14185.
9. B. Pan, F. Chen, B. Kou, J. Wang, Q. Tang, L. Guo, Q. Wang, Z. Li, W. Bian and J. Wang, *Nanoscale*, 2020, **12**, 11659-11671.
10. Q. Wang, F. Chen, Q. Tang, L. Guo, T. T. Gebremariam, T. Jin, H. Liu, B. Kou, Z. Li and W. Bian, *Applied Catalysis B: Environmental*, 2020, **270**, 118861.
11. Y. Jin, F. Chen, L. Guo, J. Wang, B. Kou, T. Jin and H. Liu, *ACS Applied Materials & Interfaces*, 2020, **12**, 26694-26703.
12. T. T. Gebremariam, F. Chen, B. Kou, L. Guo, B. Pan, Q. Wang, Z. Li and W. Bian, *Electrochimica Acta*, 2020, **354**, 136678.
13. Y. Jin, F. Chen, T. Jin, L. Guo and J. Wang, *J. Mater. Chem. A*, 2020, **8**, 25780-25790.
14. Q. Wang, F. Chen, Q. Tang, L. Guo, T. Jin, B. Pan, J. Wang, Z. Li, B. Kou and W. Bian, *Nano Research*, 2020, DOI: 10.1007/s12274-020-3220-z.
15. Q. Tang, F. Chen, T. Jin, L. Guo, Q. Wang and H. Liu, *J. Mater. Chem. A*, 2019, **7**, 22996-23007.
16. S. Sankar, G. M. Anilkumar, T. Tamaki and T. Yamaguchi, *ACS Applied Energy Materials*, 2018, **1**, 4140-4149.
17. S. Sankar, G. M. Anilkumar, T. Tamaki and T. Yamaguchi, *ChemCatChem*, 2019, **11**, 4731-4737.
18. J. Bai, Q. Xue, Y. Zhao, J.-X. Jiang, J.-H. Zeng, S.-B. Yin and Y. Chen, *ACS Sustainable Chemistry & Engineering*, 2019, **7**, 2830-2836.
19. S.-H. Han, H.-M. Liu, J. Bai, X. L. Tian, B. Y. Xia, J.-H. Zeng, J.-X. Jiang and Y. Chen, *ACS Applied Energy Materials*, 2018, **1**, 1252-1258.
20. M. Schalenbach, O. Kasian, M. Ledendecker, F. D. Speck, A. M. Mingers, K. J. J. Mayrhofer and S. Cherevko, *Electrocatalysis*, 2018, **9**, 153-161.